



# Sustain and Address Discharge Characteristics of AC-PDP with MgO Surface Coated by MgO Nano Crystal Powders

J. H. Kim<sup>1</sup>, G.-S. Park<sup>1</sup>, H. D. Park<sup>2</sup>, H.-S. Tae<sup>1,\*</sup>, and S.-H. Lee<sup>3</sup>

<sup>1</sup>School of Electronics Engineering, College of IT Engineering, Kyungpook National University, Daegu, 702-701, Korea

<sup>2</sup>Radiation Instrumentation Research Division, Korea Atomic Energy Research Institute, Daejeon, 305-353, Korea

<sup>3</sup>School of Electrical Engineering, College of Information Technology and Engineering, Inha University, Incheon, 402-751, Korea

This paper examined the sustain and address discharge characteristics of ac-PDPs with MgO surface coated by MgO nano crystal powders. The MgO nano crystal powder was deposited by about 5% on the MgO surface by using the spray method. To investigate the effects of the partial addition of MgO nano crystal powders on the sustain discharge as well as the address discharge, the luminance, IR spectra of 823, 828 nm, cathodoluminescence, and firing voltage were measured with the measurement of the address delay times and wall voltage variation in the 42-inch ac-PDP module with a high Xe content of 17%. As a result, the statistical delay characteristics were improved considerably especially under the low panel temperature of  $-5^{\circ}\text{C}$  for the MgO surface with MgO nano crystal powder. However, both MgO surfaces with and without the MgO nano crystal powder showed almost similar sustain and address discharge characteristics except the statistical delay characteristics.

**Keywords:** 42-Inch AC-PDP Module, High Xe, Functional Layer, MgO Nano Crystal Powder, Statistical Delay Time, Panel Temperature.

## 1. INTRODUCTION

An MgO layer in ac-PDP plays an important role in producing the sustain and address discharge by lowering the firing voltage thanks to its high secondary electron emission coefficient. As the size of PDPs is becoming larger and their cell numbers are increased considerably, the importance of address discharge is more emphasized under the ADS driving method, thereby requiring the better performance of MgO layer.<sup>1</sup> In particular, the fast address discharge characteristics of MgO layer are required.<sup>2</sup> Furthermore, the fast address discharge characteristics of MgO layer should be maintained under the variation in the panel temperature.

However, the conventional MgO layer is very sensitive to the variation in the panel temperature, meaning that the address discharge characteristics are quite different depending on the panel temperature. That is, in case of the conventional MgO layer, the address discharge is very unstable, and the formative and statistical delay times

are very long under the low panel temperature, whereas the formative and statistical delay times are very short and misfiring discharges are produced easily under the high panel temperature.

Recently, in order to compensate the demerit of the conventional MgO layer, various types of MgO crystal powders were used as a functional layer for improving the address delay characteristics and simultaneously lowering the firing voltage in the mini-test panel.<sup>3-7</sup>

However, in this case, the partial addition of the MgO crystal powders, particularly the few percent spray-coated MgO crystal powders, might cause a misfiring discharge because the partial addition of the MgO crystal powders might not guarantee the uniform discharge of the entire PDP panel, especially the large size (> 42-inch) panel. Accordingly, the effects of the partial addition of MgO nano crystal powders on the discharge uniformity need to be investigated under the large size PDP condition.

In this paper, to investigate the effects of the partial (5%) addition of MgO nano crystal powder sprayed on the conventional MgO surface on both the sustain and address discharge characteristics, the luminance, IR spectra of 823,

\* Author to whom correspondence should be addressed.

828 nm, and firing voltage were measured with the measurement of the address delay times and wall voltage variation in the 42-inch PDP module with a high Xe content of 17%. All these experiments were carried out under the full driving scheme with 11 subfields. In particular, the panel temperature was varied from  $-5\text{ }^{\circ}\text{C}$  to  $+65\text{ }^{\circ}\text{C}$  so as to examine the temperature dependence of the MgO nano crystal powders. The address and sustain discharge characteristics were analyzed and compared relative to the panel temperature for both the MgO layers with and without MgO nano crystal powders.

## 2. EXPERIMENTAL SETUP

Figure 1(a) shows the conventional MgO surface grown by using the ion plating method, whereas Figure 1(b) shows the MgO nano crystal powders coated on the conventional MgO surface by using the spray method. As shown in the SEM image of Figure 1(b), the MgO nano crystal powders had sizes ranging from a few tens of nanometers to a few micrometers, and the big size of the MgO crystal powder showed the cubic shape.

In this experiment, the MgO nano crystal powders had a five percent deposited area over the entire MgO surface. The HD grade 42-inch ac-PDP modules were used as test panels in which all the PDP cell conditions were exactly the same, except the MgO surfaces with and without MgO nano crystal powders, as shown in Table I. Figures 2(a) and (b) show the schematic diagrams of the measurement system and related voltage driving waveforms employed in this research. In Figure 2(a), the infrared (IR) emissions were measured by using the spectrometer and photosensor amplifier (Hamamatsu, C6386), and the luminance was

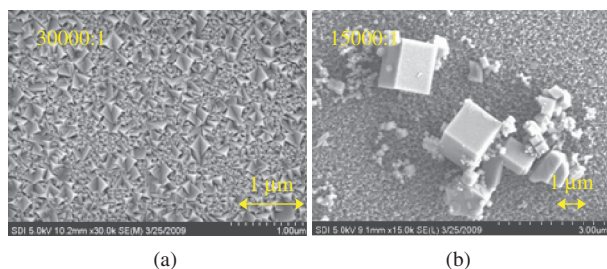


**Fig. 1.** Comparison of SEM images of MgO surfaces (a) without and (b) with MgO nano crystal powders. The sizes of MgO nano crystal powders range from a few tens of nanometers to a few micrometers.

**Table I.** Specifications of 42-inch ac-PDP used in this study.

Front panel		Rear panel	
ITO width	200 $\mu\text{m}$	Barrier rib width	60 $\mu\text{m}$
ITO gap	70 $\mu\text{m}$	Barrier rib height	120 $\mu\text{m}$
Bus width	50 $\mu\text{m}$	Address width	90 $\mu\text{m}$
Cell pitch	912 $\mu\text{m}$ $\times$ 692 $\mu\text{m}$		
Gas composition	Ne-Xe (17%)-He (60%)		
Panel pressure	420 Torr		

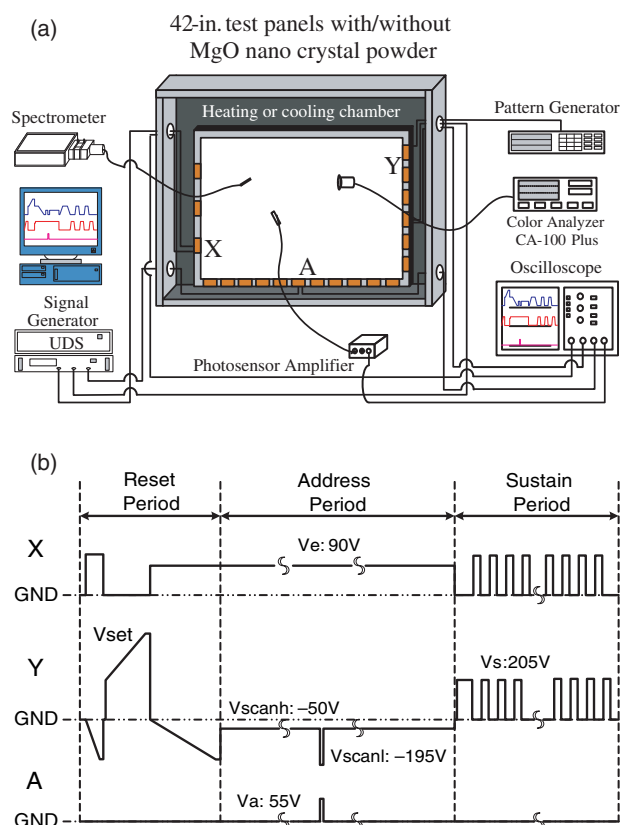


**Fig. 2.** Schematic diagrams of (a) measurement system and (b) voltage driving waveform used in this study.

measured by using the luminance analysis (CA-100 Plus). As shown in Figure 2(b), the address voltage of 55 V, the scan high ( $= V_{\text{scanh}}$ ) of  $-50\text{ V}$ , and the scan low ( $= V_{\text{scanl}}$ ) voltages of  $-195\text{ V}$  were applied during the address period, whereas the sustain voltage of 205 V was applied under a driving frequency of 200 kHz during the sustain period.

## 3. RESULTS AND DISCUSSION

### 3.1. Measurements of Firing Voltage and Cathodoluminescence (CL) Related to Sustain Discharge Characteristics

Figure 3 shows the  $V_i$  closed curves measured from the 42-inch test panels with and without MgO nano crystal powders on the MgO protective layers. Table III shows the values of firing voltages obtained from the  $V_i$  closed curves of Figure 3. Figure 3 and Table II show that the firing voltages were almost similar irrespective of the presence of the MgO nano crystal powders, implying the 5% addition of MgO nano crystal powders on the MgO surface did not affect the variation of the firing voltage.

Figure 4 shows the cathodoluminescence (CL) intensities measured from the 42-inch test panels with and without MgO nano crystal powders on the MgO protective layers.

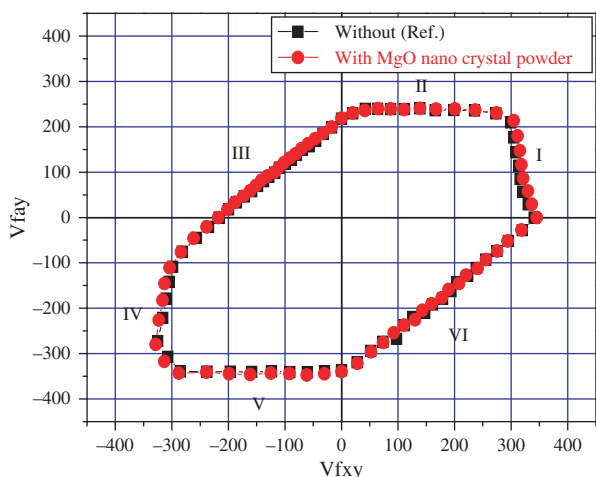


**Fig. 3.**  $V_i$  closed curves measured from 42-inch test panels with and without MgO nano crystal powders on MgO protective layers where side I is firing voltage between X–Y electrodes, side II is firing voltage between A–Y electrodes, side III is firing voltage between A–X electrodes, side IV is firing voltage between Y–X electrodes, side V is firing voltage between Y–A electrodes, and side VI is firing voltage between X–A electrodes.

**Table II.** Firing voltages measured from 42-inch test panels with and without MgO nano crystal powder on MgO protective layers.

Region	Firing voltage	
	Without (ref.) (V)	With MgO nano crystal powder (V)
MgO cathode		
I	307	314
II	238	239
III	219	221
IV	306	313
Phosphor cathode		
V	341	346
VI	353	352

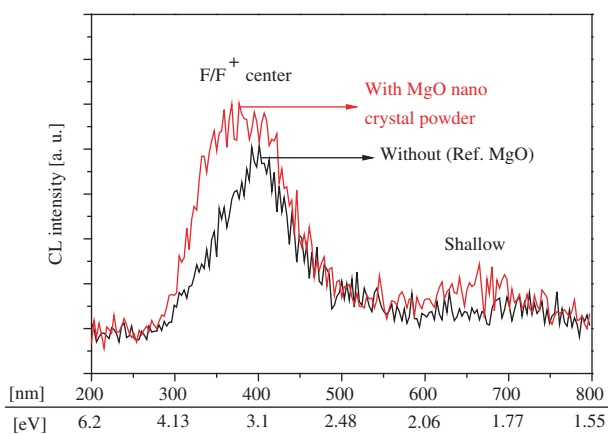


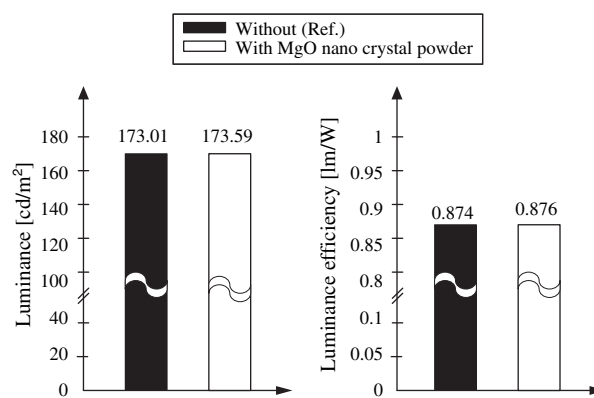
**Fig. 4.** Comparison of CL intensity with/without MgO nano crystal powders on MgO layer in 42-inch ac-PDP.

Of the two peaks in the CL intensity shown in Figure 4, the one peak meant the  $F/F^+$  center peaks positioned at about 2.5–4.1 eV that was related to the secondary electron emission, whereas the other peak meant the shallow peak positioned at about 1–2 eV that was related to the emission of electrons trapped in the low energy level of the MgO.<sup>8,9</sup> The CL measurement data in Figure 4 illustrate that the 5% coating of the MgO nano crystal powders on the MgO surface can induce the increase in the  $F/F^+$  center peaks at about 3–4 eV as well as the shallow peak at about 1–2 eV. Nonetheless, as shown in Figure 3, the changes in the deep energy level ranging from 2.5 to 4.1 eV did not reduce the firing voltage. Our experimental results of Figures 3 and 4 showed the tendency contradictory to the results that the  $F/F^+$  center peaks at about 2.5–4.1 eV was related to the secondary electron emission.

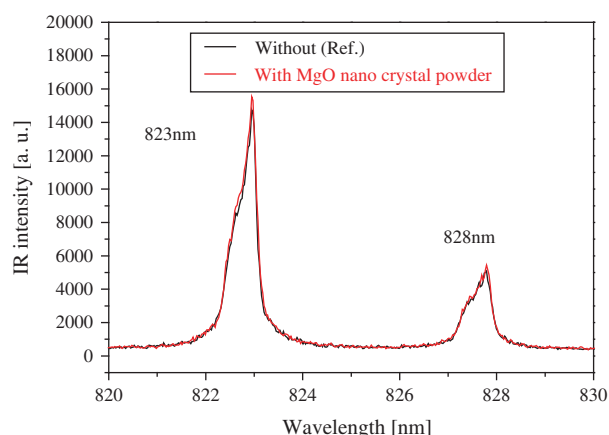
### 3.2. Measurements of Luminance, Luminous Efficiency and IR Spectrum Related to Sustain Discharge Characteristics

Figure 5 shows the luminance and luminous efficiency measured from the 42-inch test panels with and without MgO nano crystal powders on the MgO protective layers. The driving conditions for measurement were as follows: under the full-white pattern, the sustain voltage was 205 V and the 64 sustain pulses were applied during the sustain period. Like the firing voltage case of Figure 3, the luminance and luminous efficiency were almost similar irrespective of the presence of the MgO nano crystal powders, implying the 5% addition of MgO nano crystal powders on the MgO surface did not affect the variation of the luminance and luminous efficiency.

Figure 6 shows the IR emission intensities of 823 and 828 nm measured from the 42-inch test panels with and without MgO nano crystal powders on MgO protective layers. As shown in Figure 6, both cases, i.e., with and without MgO nano crystal powders, showed almost the same emission intensities for the IR of 823 and 828 nm



**Fig. 5.** Comparison of luminance and luminous efficiency measured from 42-inch test panels with and without MgO nano crystal powders on MgO protective layers.



**Fig. 6.** Comparison of IR emission intensities (823 and 828 nm) measured from 42-inch test panels with and without MgO nano crystal powders on MgO protective layers.

which eventually emit the vacuum ultraviolet of 147 and 173 nm. This result also illustrates that the IR emission characteristics strongly depends on the MgO surface characteristics instead of the MgO nano crystal powders.

### 3.3. Measurement of Address Delay Time and Wall Voltage Variation Related to Address Discharge Characteristics

Figure 7 shows the changes in the address delay times measured at room panel temperature from the 42-inch test panels with and without MgO nano crystal powders on MgO protective layers. For the red, green, and blue cells with MgO surfaces coated by the MgO nano crystal powders, the formative delay time ( $= T_f$ ) was decreased slightly, whereas the statistical delay time ( $= T_s$ ) was decreased considerably. This experimental result confirms that the partial addition of the MgO nano crystal powders

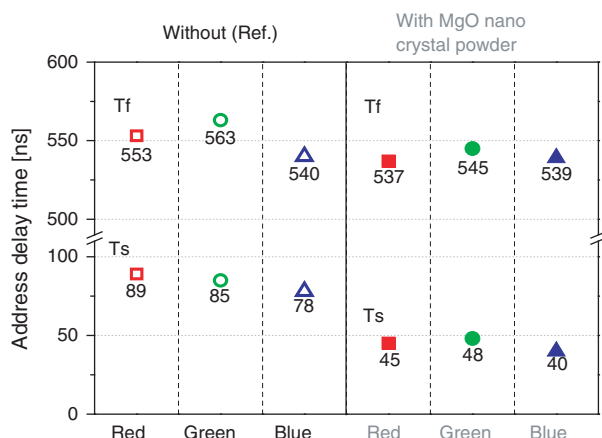


**Fig. 7.** Comparison of address delay times measured at room panel temperature from red, green, and blue cells of 42-inch test panels with and without MgO nano crystal powders on MgO protective layers where  $T_f$  is formative delay time and  $T_s$  is statistical delay time.

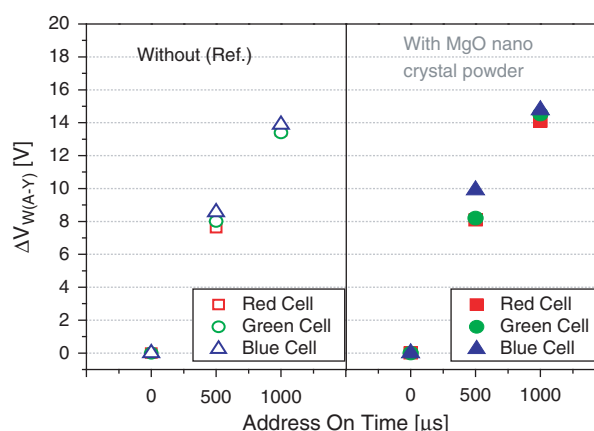


**Fig. 8.** Comparison of wall voltage variation with/without MgO nano crystal powder on MgO layer in 42-inch ac-PDP.

on the MgO surface contributes to reducing the  $T_s$  instead of  $T_f$ .

Figure 8 shows the wall voltage variations for both cases, i.e., with and without MgO nano crystal powders, relative to the address-on-time during the address period. For the conventional MgO case, the wall voltage variations were increased with an increase in the address-on-time. This tendency was observed to remain for the MgO nano crystal powders. In general, it has been known that in case of shortening the statistical delay time for the conventional MgO surface, the corresponding wall voltage variation was increased considerably.<sup>10-12</sup>

However, in case of shortening the statistical delay time using the MgO nano crystal powders, the corresponding wall voltage was not aggravated largely. Accordingly, this result confirms that the use of the MgO nano crystal powders as a functional layer contributes to enhancing the address discharge characteristics.

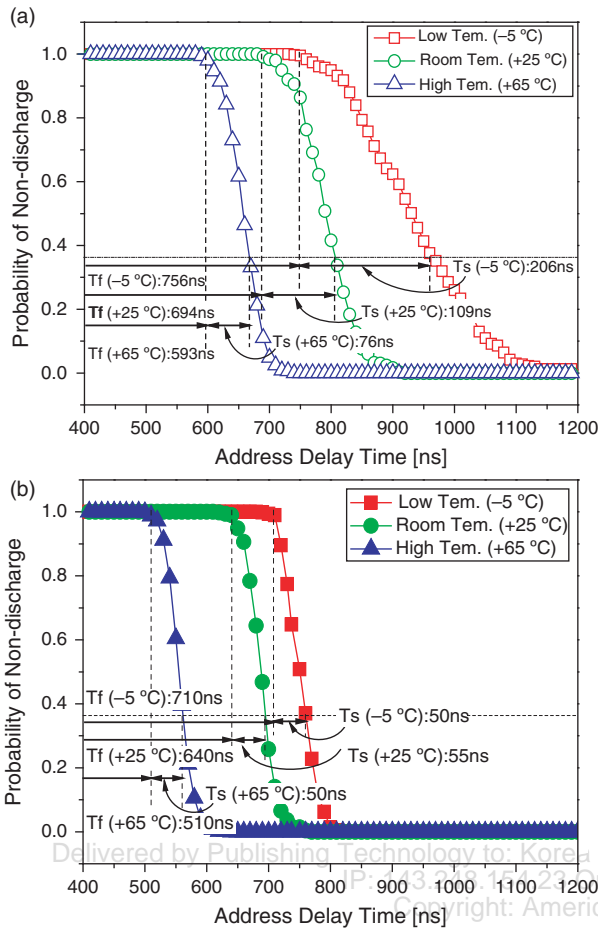
### 3.4. Variation of Address Delay Times Relative to Panel Temperatures

Figure 9 and Table III show the changes in the Laue plots of address delay times and statistical delay time measured under three different panel temperatures ( $-5$ ,  $+25$ , and  $+65$  °C) from the 42-inch test panels (a) without MgO nano crystal powder and (b) with MgO nano crystal powders.

The formative ( $T_f$ ) and statistical ( $T_s$ ) delay times were obtained by using the following equation of (1) based on the Laue plots of Figure 9.<sup>13</sup>

$$\begin{aligned}
 & \text{Probability of non-discharge } (P) \\
 & = \exp[-(t - T_f)/T_s] \quad \text{for } (t \geq T_f) \\
 & = 1 \quad \text{for } (0 \leq t \leq T_f)
 \end{aligned} \tag{1}$$

Where,  $T_f$  is a formative delay time, and  $T_s$  is a statistical delay time. In Eq. (1),  $P = 1$  means that the address



**Fig. 9.** Laue plots of address delay times measured under three different panel temperature conditions such as  $-5$ ,  $+25$ , and  $+65$  °C from 42-inch test panels (a) without MgO nano crystal powder and (b) with MgO nano crystal powders.

discharge is not produced, whereas  $P = 0$  is the address discharge is produced stably. For the conventional MgO surface, the address delay times were increased from 76 to 206 ns as the panel temperature was lowered from  $+65$  to  $-5$  °C. It has been known that the address delay characteristics strongly depend on the presence of the exo-electrons emitted from the MgO surface as a result of thermal excitation.<sup>14-16</sup>

Accordingly, under the low panel temperature of  $-5$  °C, the emission characteristics of exo-electrons from the MgO surface was reduced considerably, thereby resulting in

**Table III.** Statistical address delay times measured under three different panel temperature conditions such as  $-5$ ,  $+25$ , and  $+65$  °C from 42-inch test panels without MgO nano crystal powder and with MgO nano crystal powders.

	Without (Ref.) (ns)	With MgO nano crystal powder (ns)
Low temperature ( $-5$ °C)	206	50
Room temperature ( $+25$ °C)	109	55
High temperature ( $+65$ °C)	76	50

aggravating the address delay characteristics, especially the statistical delay characteristics. However, as shown in Figure 9(b), for the MgO surface coated by the MgO nano crystal powders, the address delay time, especially statistical delay time was changed very slightly despite the low panel temperature of  $-5$  °C. As shown in Figure 9(b), the PDP cells with the MgO surface coated by the MgO nano crystal powders showed the statistical delay characteristics independent of the panel temperature.

This result would postulate that unlike the conventional MgO surface, there would be an electron emission from the MgO nano crystal powders irrespective of the panel temperature variation. We can deduce from the CL data of the MgO nano crystal powders in Figure 4 that the seed electrons could be provided by the emission of the electrons trapped in the  $F/F^+$  center and shallow energy level. However, this point remains still unclear, requiring the further study.

#### 4. CONCLUSION

In this paper, the sustain and address discharge characteristics of ac-PDPs having the MgO surface with and without MgO nano crystal powders were compared and examined. Under the 42-inch ac-PDP module with a high Xe content of 17%, the luminance, IR spectra of 823, 828 nm, CL intensity, and firing voltage related to the sustain discharge characteristics were measured, and the address delay times and wall voltage variation related to the address discharge characteristics were measured.

For the MgO surface with MgO nano crystal powder, the statistical delay characteristics were improved considerably especially under the low panel temperature of  $-5$  °C. However, both MgO surfaces with and without the MgO nano crystal powder showed almost similar sustain and address discharge characteristics except the statistical delay characteristics.

**Acknowledgment:** This work was supported by Kyungpook National University Research Fund, 2012.

#### References and Notes

1. K.-H. Park, H.-S. Tae, and J. H. Seo, *IEEE Trans. Plasma Sci.* 38, 3128 (2010).
2. J. S. Kim, J. H. Yang, and K. W. Whang, *IEEE Trans. Electron Devices* 51, 548 (2004).
3. T. Okada, T. Naoi, and T. Yoshioka, *J. Appl. Phys.* 105, 113304 (2009).
4. T. Naoi, H. Lin, A. Hirota, E. Otani, and K. Amemiya, *J. Soc. Inf. Disp.* 17, 113 (2009).
5. J.-S. Choe, S.-H. Moon, J.-H. Kim, and G.-H. Kim, *Current Appl. Phys.* 10, 1378 (2010).
6. K. Hashimoto, S. Itakura, K. Sakata, T. Tokunaga, M. Ishizuka, S. Iwaoka, and N. Saegusa, *J. Soc. Inf. Disp.* 17, 107 (2009).
7. M. S. Chung, M. J. Jeon, S. C. Lee, B. K. Kang, H. J. Kim, S. S. Yang, J. S. Kim, and Y. J. Ahn, *Displays* 28, 68 (2007).

8. C.-S. Park and H.-S. Tae, *IEEE Trans. Plasma Sci.* 38, 2439 (2010).
9. Y. Motoyama, Y. Hirano, K. Ishii, Y. Murakami, and F. Sato, *J. Appl. Phys.* 95, 8419 (2004).
10. C.-R. Hong, S.-H. Yoon, and Y.-S. Kim, *Thin Solid Films* 517, 4170 (2009).
11. S.-K. Jang, C.-S. Park, H.-S. Tae, B. J. Shin, J. H. Seo, and E.-Y. Jung, *J. Soc. Inf. Disp.* 18, 614 (2010).
12. B.-T. Choi, H. D. Park, and H.-S. Tae, *IEICE Trans. Electron.* E92-C, 1347 (2009).
13. N. Uemura, Y. Yajima, M. Shibata, Y. Kawanami, and F. Namiki, *SID Int. Symp. Dig. Tech. Pap.* 34, 784 (2003).
14. S.-H. Yoon, C.-R. Hong, J. J. Ko, H.-S. Yang, and Y.-S. Kim, *J. Soc. Inf. Disp.* 12, 131 (2009).
15. H. Tolner, *Proc. of ASID'06 Dig.* (2006), p. 136.
16. S.-K. Jang and H.-S. Tae, *IEEE Trans. Plasma Sci.* 18, 334 (2009).

Received: 25 January 2012. Accepted: 9 June 2012.

Delivered by Publishing Technology to: Korea Advanced Institute of Science & Technology (KAIST)  
IP: 143.248.154.23 On: Fri, 14 Feb 2014 06:13:50  
Copyright: American Scientific Publishers

RESEARCH ARTICLE